



ON THE APPLICATION OF KINETIC THEORY TO GRANULAR GASES



Vicente Garzó

Departamento de Física and ICCAEx, Universidad de Extremadura,
Badajoz, Spain



Fondo Europeo de
Desarrollo Regional
“Una manera de hacer Europa”

Grant PID2020-112936GB-I00

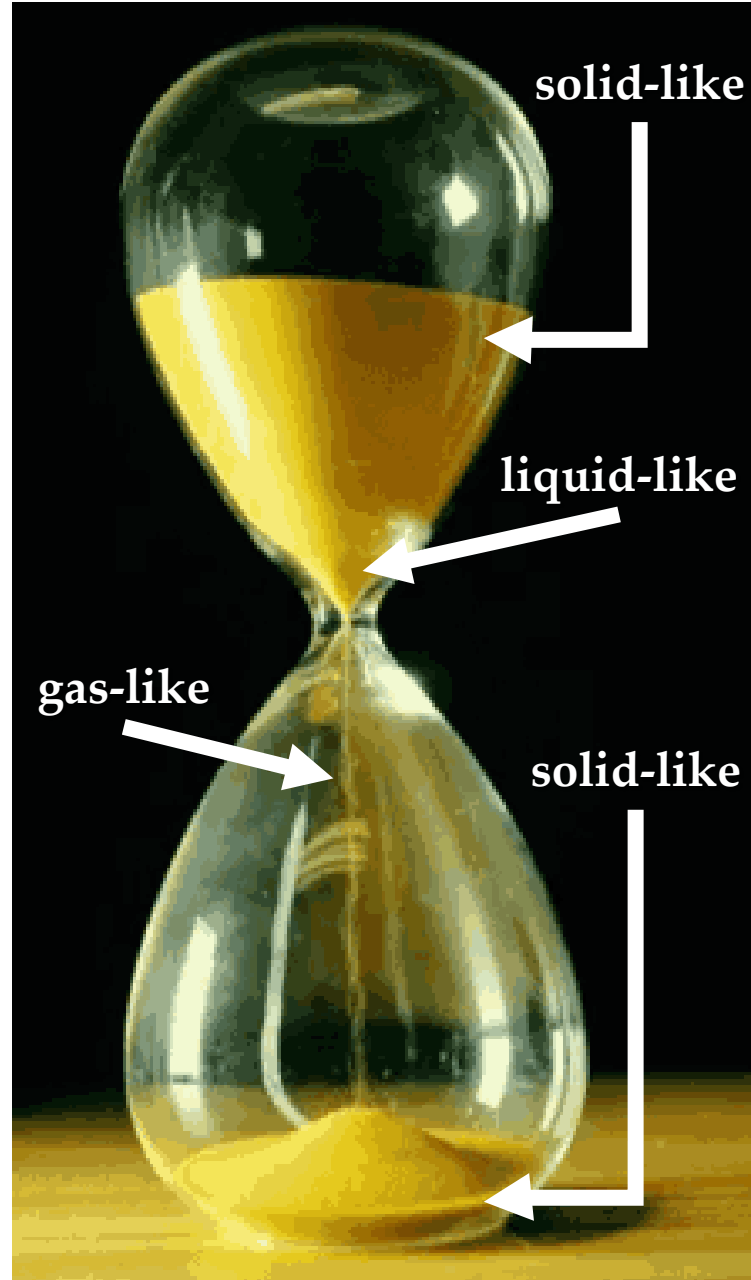
FisES'23, Pamplona, 25-27 Octubre 2023

OUTLINE

1. Granular monocomponent gases. Inelastic Enskog kinetic equation.
Some applications
2. Granular mixtures: Tracer limit. Some applications
3. Random walk connection
4. Conclusions and perspectives

Granular matter

- Large collections of discrete and macroscopic particles.
- Sizes from $\sim 1 \mu\text{m}$ to $\sim 10^3 \text{ km}$.
- Macroscopic \rightarrow dissipative interactions.
- Different phases that recalls the states of matter.
- Very present in geophysical processes and astrophysical systems.
- Second most-used material in industry after water. [V. Folli et al., *Sci. Rep.* **3** (2013)]



Activated: External energy compensates for the energy dissipated by collisions and effects of gravity

Rapid flow conditions: motion of grains is similar to motion of molecules or atoms in a classical gas. They behave like a fluid and flow. Hydrodynamic-like description. **Dry granular gas** (No interstitial fluid)

Simplest microscopic model: *smooth inelastic hard spheres*

Smooth hard spheres
with *inelastic* collisions

$$(\mathbf{g}'_{12} \cdot \hat{\boldsymbol{\sigma}}) = -\alpha (\mathbf{g}_{12} \cdot \hat{\boldsymbol{\sigma}})$$

Coefficient of restitution

$$0 < \alpha \leq 1$$

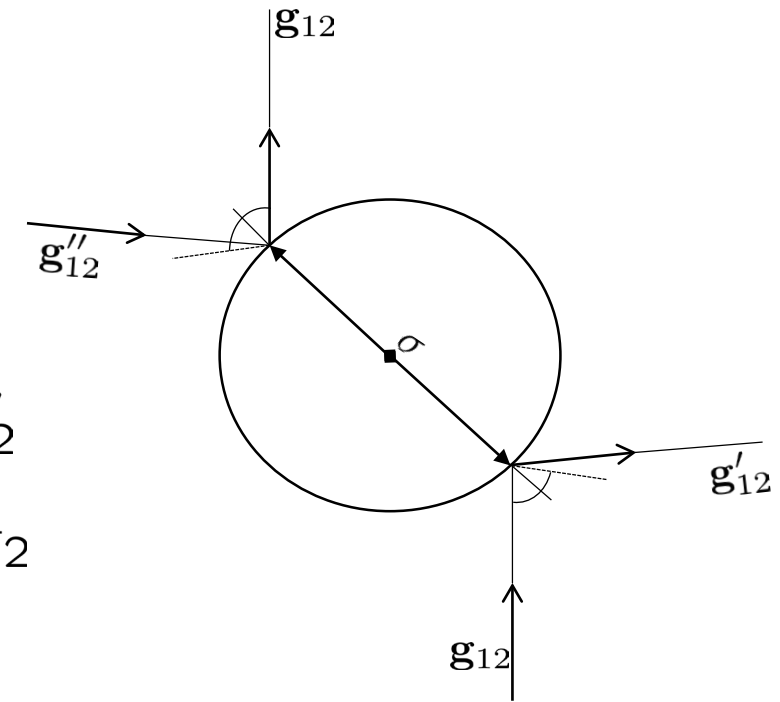
$$\mathbf{g}'_{12} = \mathbf{v}'_1 - \mathbf{v}'_2$$

$$\mathbf{g}_{12} = \mathbf{v}_1 - \mathbf{v}_2$$

Direct collision

$$\mathbf{v}'_1 = \mathbf{v}_1 - \frac{1}{2} (1 + \alpha) (\hat{\boldsymbol{\sigma}} \cdot \mathbf{g}_{12}) \hat{\boldsymbol{\sigma}}$$

$$\mathbf{v}'_2 = \mathbf{v}_2 + \frac{1}{2} (1 + \alpha) (\hat{\boldsymbol{\sigma}} \cdot \mathbf{g}_{12}) \hat{\boldsymbol{\sigma}}$$



Momentum conservation

$$v_1 + v_2 = v'_1 + v'_2$$

Collisional energy change

$$\Delta E = \frac{1}{2}m(v'^2_1 + v'^2_2 - v^2_1 - v^2_2) = -\frac{m}{4}(1 - \alpha^2)(g_{12} \cdot \hat{\sigma})^2$$

Very **simple** model that *captures* many properties of granular flows,
especially those associated with dissipation

KINETIC DESCRIPTION

One-particle velocity distribution function

Average number of particles at
 $f(\mathbf{r}, \mathbf{v}, t) d\mathbf{r} d\mathbf{v} \rightarrow t$ located around \mathbf{r} and moving with \mathbf{v}

Moderately dense gas: fraction of the volume occupied by granular material is not negligible compared to the total volume

Enskog kinetic equation

- *Spatial correlations (volume excluded effects)*
- “*Molecular chaos*”

Limitation: Velocity correlations are still neglected
(molecular chaos hypothesis) !!

Baxter, Olafsen PRL **99**, 028001 (2007)

$$\partial_t f + \mathbf{v} \cdot \nabla f + \mathbf{g} \cdot \frac{\partial f}{\partial \mathbf{v}} = J_E [\mathbf{r}, \mathbf{v} | f(t), f(t)]$$

$$\begin{aligned} J_E(\mathbf{r}_1, \mathbf{v}_1; t) &= \sigma^{d-1} \int d\mathbf{v}_2 \int d\hat{\boldsymbol{\sigma}} \Theta(\hat{\boldsymbol{\sigma}} \cdot \mathbf{g}_{12})(\hat{\boldsymbol{\sigma}} \cdot \mathbf{g}_{12}) \\ &\times \left(\alpha^{-2} \mathbf{f}_2(\mathbf{r}_1, \mathbf{v}_1'', \mathbf{r}_1 - \boldsymbol{\sigma}, \mathbf{v}_2''; t) - \mathbf{f}_2(\mathbf{r}_1, \mathbf{v}_1, \mathbf{r}_1 + \boldsymbol{\sigma}, \mathbf{v}_2; t) \right) \end{aligned}$$

$$f_2(\mathbf{r}_1, \mathbf{v}_1, \mathbf{r}_2, \mathbf{v}_2; t) = \chi(\mathbf{r}_1, \mathbf{r}_2) f(\mathbf{r}_1, \mathbf{v}_1; t) f(\mathbf{r}_2, \mathbf{v}_2; t)$$

Pair correlation function

N. Brilliantov, T. Pöschel, *Kinetic Theory of Granular Gases* (OUP, 2004); VG, *Granular Gaseous Flows* (Springer, 2019)

Hydrodynamic fields

Number density $n(\mathbf{r}, t) = \int d\mathbf{v} f(\mathbf{r}, \mathbf{v}; t)$

Flow velocity $\mathbf{U}(\mathbf{r}, t) = \frac{1}{n(\mathbf{r}, t)} \int d\mathbf{v} \mathbf{v} f(\mathbf{r}, \mathbf{v}; t)$

Granular **temperature** $T(\mathbf{r}, t) = \frac{1}{dn(\mathbf{r}, t)} \int d\mathbf{v} m[\mathbf{v} - \mathbf{U}(\mathbf{r}, t)]^2 f(\mathbf{r}, \mathbf{v}; t)$

$$D_t n + n \nabla \cdot \mathbf{U} = 0$$

$$D_t \mathbf{U} + \rho^{-1} \nabla \cdot \mathbf{P} = \mathbf{g}$$

$$\frac{d}{2} n D_t T + \nabla \cdot \mathbf{q} + \mathbf{P} : \nabla \mathbf{U} = -\frac{d}{2} n T \zeta$$

$$D_t \equiv \partial_t + \mathbf{U} \cdot \nabla$$

Cooling rate: Provides the energy loss rate due to inelastic collisions

$$\begin{aligned} \zeta &= (1 - \alpha^2) \frac{m \sigma^{d-1}}{4 d n T} \int d\mathbf{v}_1 \int d\mathbf{v}_2 \int d\hat{\boldsymbol{\sigma}} \Theta(\hat{\boldsymbol{\sigma}} \cdot \mathbf{g}_{12}) (\hat{\boldsymbol{\sigma}} \cdot \mathbf{g}_{12})^3 \\ &\quad \times \chi(\mathbf{r}, \mathbf{r} + \boldsymbol{\sigma}) f(\mathbf{r}, \mathbf{v}_1; t) f(\mathbf{r} + \boldsymbol{\sigma}, \mathbf{v}_2; t) \end{aligned}$$

CHAPMAN-ENSKOG NORMAL SOLUTION

Assumption: For long times (much longer than the mean free time) and far away from boundaries (bulk region) the system reaches a **hydrodynamic** regime.

Normal solution $f(\mathbf{r}, \mathbf{v}; t) = f[\mathbf{v}|n(\mathbf{r}, t), \mathbf{U}(\mathbf{r}, t), T(\mathbf{r}, t)]$

In some situations, gradients are controlled by boundary or initial conditions. Small spatial gradients:

$$f = f^{(0)} + f^{(1)} + \dots$$

Homogeneous **cooling** state (HCS)

Some *controversy* about the possibility of going from kinetic theory to hydrodynamics by using the CE method

The **time scale** for T is set by the **cooling rate** instead of spatial gradients. In this new time scale, T is *much faster* than in the usual hydrodynamic scale.

For **large inelasticity** (ζ^{-1} small), *perhaps* there were **NO** time scale separation between hydrodynamic and kinetic excitations:
NO AGING to hydrodynamics!!

We assume the validity of a hydrodynamic description and compare with computer simulations: Monte Carlo (**DSMC**) and **MD** simulations

Constitutive equations for the fluxes and the cooling rate

Small spatial gradients (Navier-Stokes hydrodynamic order)

$$P_{ij} \rightarrow p\delta_{ij} - \eta \left(\partial_i U_j + \partial_j U_i - \frac{2}{d} \delta_{ij} \nabla \cdot \mathbf{U} \right) - \eta_b \delta_{ij} \nabla \cdot \mathbf{U}$$

$$\mathbf{q} \rightarrow -\kappa \nabla T - \mu \nabla n$$

$$\zeta \rightarrow n \sigma^{d-1} \sqrt{\frac{2T}{m}} \zeta_0^* + \zeta_U \nabla \cdot \mathbf{U}$$

Shear viscosity $\eta(\alpha, \phi) = \eta(1, 0)\eta^*(\alpha, \phi)$, $\eta(1, 0) \propto \sigma^{1-d}\sqrt{mT}$

Low-density value for elastic collisions

Bulk viscosity $\eta_b(\alpha, \phi) = \eta(1, 0)\eta_b^*(\alpha, \phi)$ $\phi = C_d n \sigma^d$

Thermal conductivity $\kappa(\alpha, \phi) = \kappa(1, 0)\kappa^*(\alpha, \phi)$, $\kappa(1, 0) \propto \eta(1, 0)/m$

Diffusive heat conductivity $\mu(\alpha, \phi) = \frac{T\kappa(1, 0)}{n}\mu^*(\alpha, \phi)$, $\mu^*(1, \phi) = 0$

First-order contribution to the cooling rate $\zeta_U(\alpha, \phi)$

Pressure $p(\alpha, \phi) = nT p^*(\alpha, \phi)$

Kinetic contributions to the reduced transport coefficients given in terms of solutions of a set of coupled linear equations. *Collisional* contributions in terms of $f^{(0)}$

Approximate expressions

- Leading terms in a Sonine (associated Laguerre) polynomial expansion.
Standard first Sonine approximation [VG, J.W. Dufty, PRE **59**, 5895 (1999);
J. F. Lutsko, PRE **72**, 021306 (2005)]
- *Modified* first Sonine approximation [VG, A. Santos, J.M. Montanero, Physica A **376**, 94 (2007)]
- *Computer*-aided method. Dilute gases
[S.H. Noskowicz, O. Bar-Lev, D. Serero, I. Goldhirsch, EPL **79**, 6001 (2007)]

For *nearly* elastic spheres but *dense* gases, we recover previous results

[J. Jenkins, S. Savage, JFM **130**, 187 (1983); J. Jenkins, M. W. Richman, Arch. Ration. Mech. Anal. **87**, 355 (1985); Phys. Fluids **28**, 3485 (1985); C.K.K. Lun et al. JFM **140**, 223 (1984); **233**, 539 (1991); A. Goldshtain, M. Shapiro, JFM **282**, 75 (1995); N. Sela, I. Goldhirsch, JFM **361**, 41 (1998)]

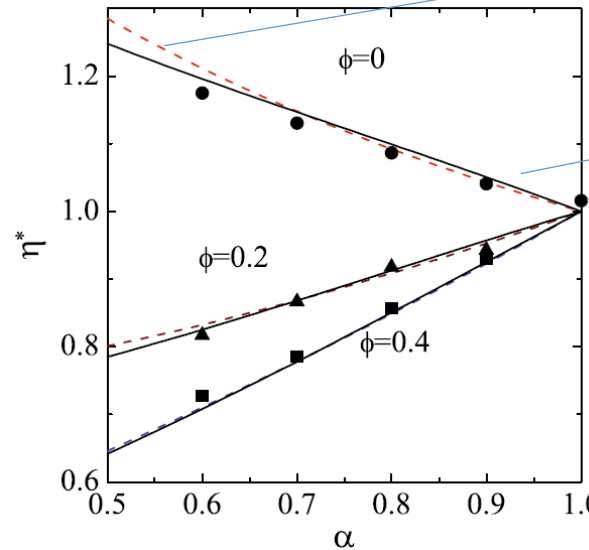
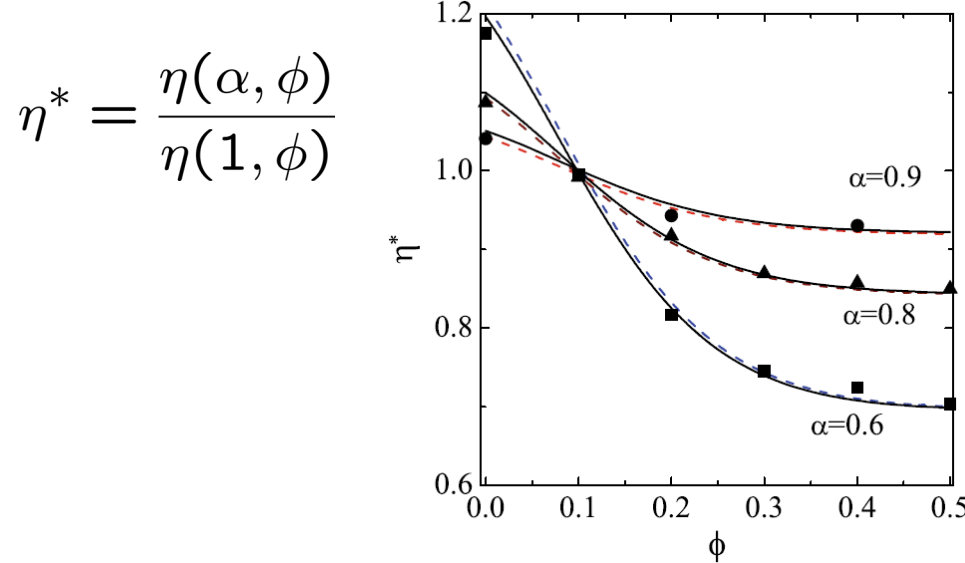
For *inelastic* spheres but *dilute* gases, we also recover previous results

[J.J. Brey, J.W. Dufty, C-S Kim, A. Santos, PRE **58**, 4638 (1998)].

Our results apply (in principle) to *arbitrary* inelasticity and *moderate* densities

Hard spheres (d=3)

Reduced shear viscosity



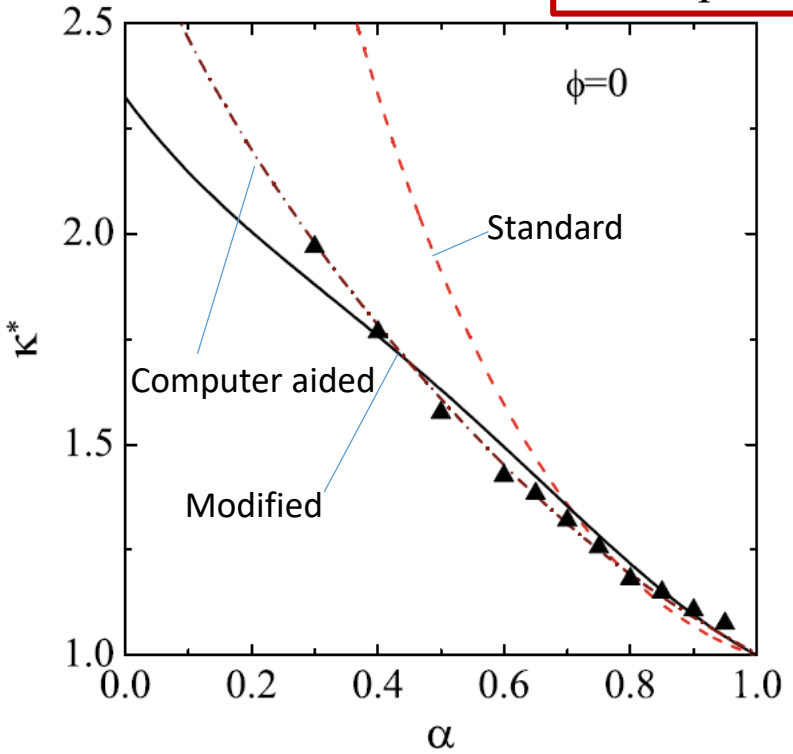
Standard Sonine approach

Modified Sonine approach

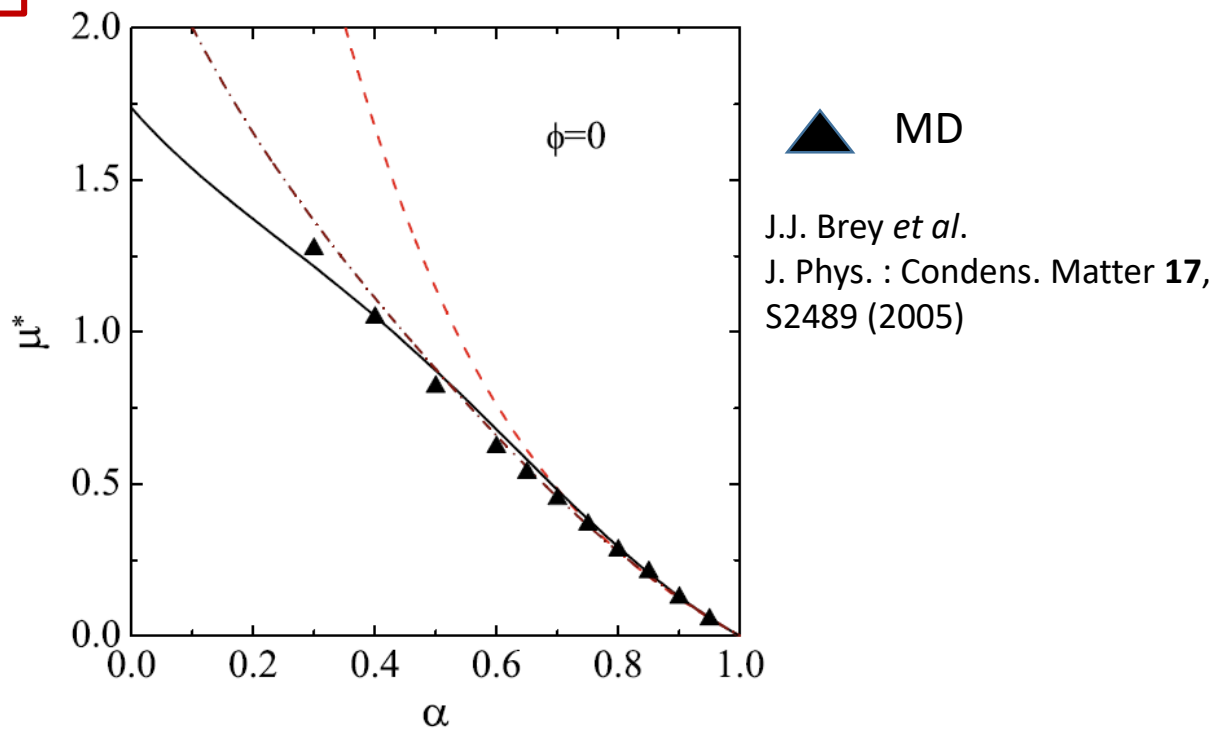
DSMC (Monte Carlo) simulations [J. M. Montanero, A. Santos, VG, AIP Conf. Proc. **762**, 797 (2005)]

Comparison between theory and Monte Carlo simulations **supports** hydrodynamic solution

Hard spheres (d=3)



$$\kappa^* = \frac{\kappa(\alpha, 0)}{\kappa(1, 0)}$$



$$\mu^* = \frac{n}{T\kappa(1, 0)}\mu(\alpha, 0)$$

Modified Sonine approach and computer-aided method compare well with MD simulations, even for quite strong inelasticity. Agreement **supports** molecular chaos hypothesis.

Stability of the homogeneous cooling state (HCS)

Spontaneous formation of velocity vortices and density clusters in HCS

VOLUME 70, NUMBER 11

PHYSICAL REVIEW LETTERS

15 MARCH 1993

Clustering Instability in Dissipative Gases

I. Goldhirsch

*Department of Fluid Mechanics and Heat Transfer, Faculty of Engineering, Tel-Aviv University,
Ramat Aviv, Tel-Aviv 69978, Israel*

G. Zanetti^(a)

*Applied & Computational Mathematics, Princeton University, Princeton, New Jersey 08544
(Received 3 September 1991)*

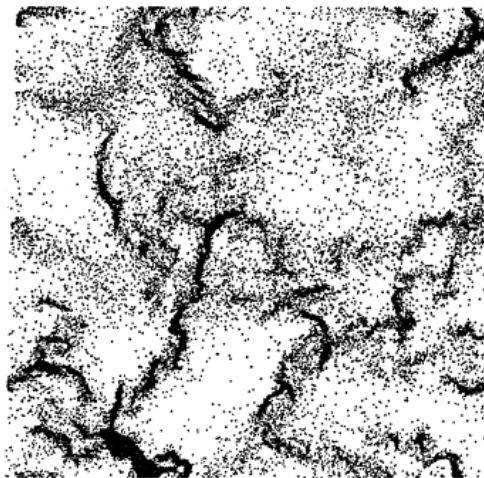


FIG. 3. A typical configuration of particles exhibiting clusters. Here the coefficient of restitution is 0.6, the time corresponds to 500 collisions per particle, and the area fraction is 0.05. The number of particles is 40000.

Hydrodynamic modes of a uniform granular medium

Sean McNamara

Scripps Institution of Oceanography, La Jolla, California 92093-0230

Phys. Fluids 5, 3056 (1993)

Origin of this instability: inelastic collisions

Very nice application of the Navier-Stokes hydrodynamics: determine the critical length L_c

System becomes **unstable** when its linear size $L > L_c$

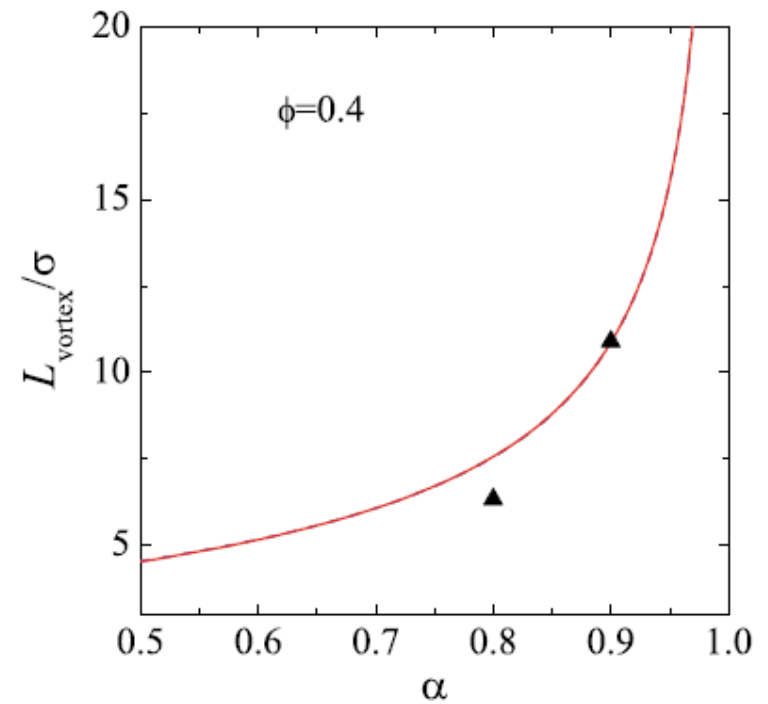
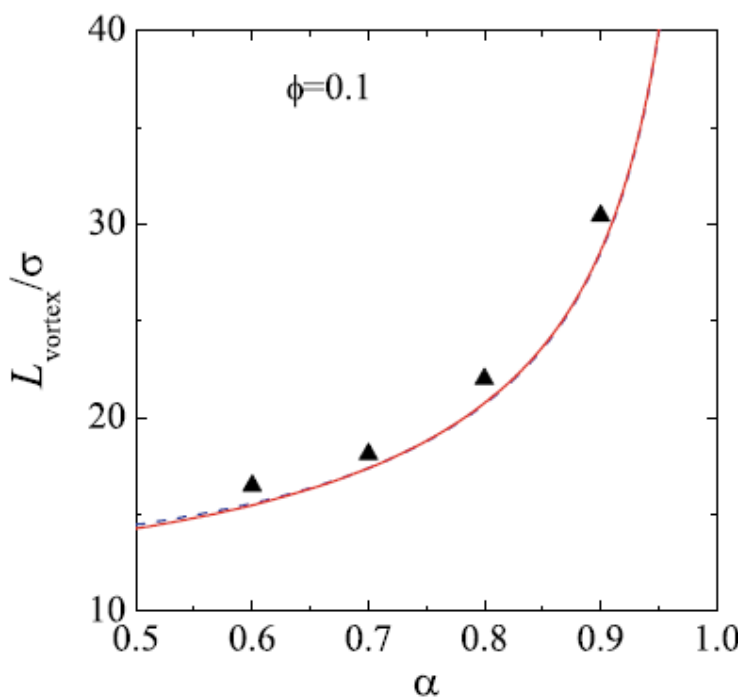
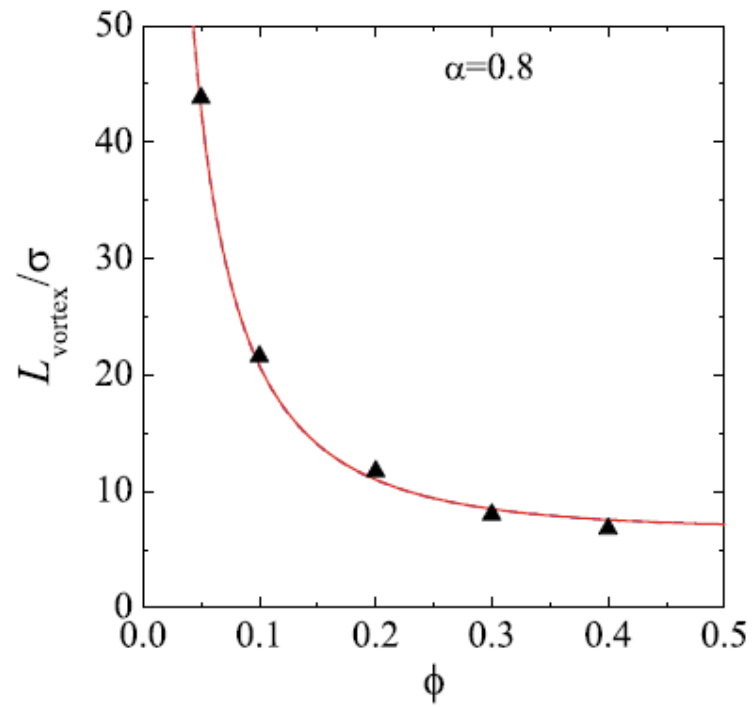
Critical size

$$\frac{L_c}{\sigma} \equiv \min \left\{ \frac{L_{\text{vortex}}}{\sigma}, \frac{L_{\text{cluster}}}{\sigma} \right\} \equiv \left\{ \frac{5\pi\sqrt{2\pi}}{48\phi} \sqrt{\frac{\eta^*}{\zeta_0^*}}, \frac{5\sqrt{5}}{48\phi} \pi^{3/2} \sqrt{\frac{\kappa^* C_\rho - \mu^*}{\zeta_0^* (2\xi - C_\rho)}} \right\} \quad d = 3$$

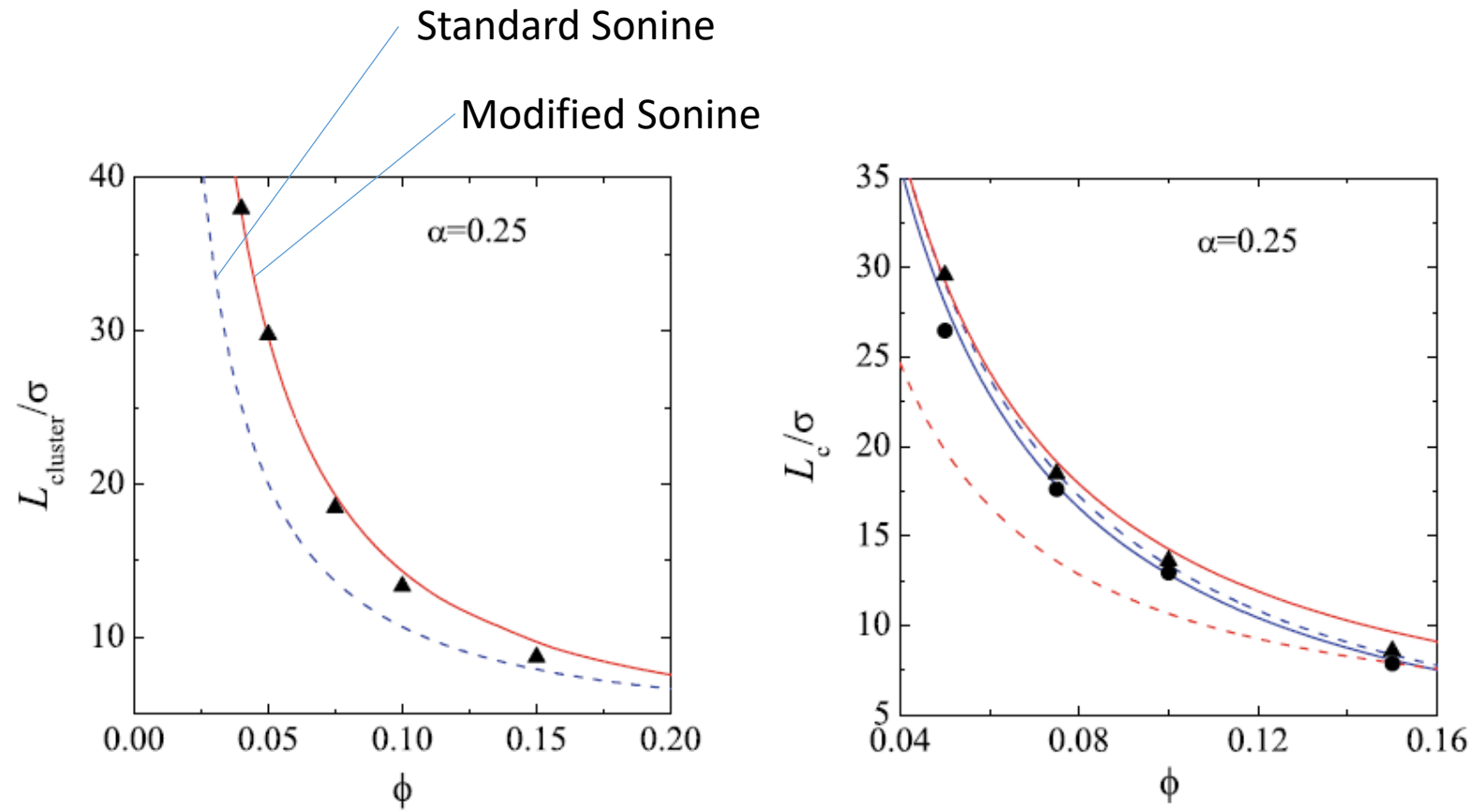
$$\xi = 1 + \phi \partial_\phi \ln \chi, \quad C_\rho = 1 + \xi - \frac{\xi}{1 + 2(1 + \alpha)\phi\chi}$$

[VG, PRE **72**, 021106 (2005)]

Comparison with MD simulations



[P. Mitrano *et al.* Phys. Fluids **23**, 093303 (2011)]

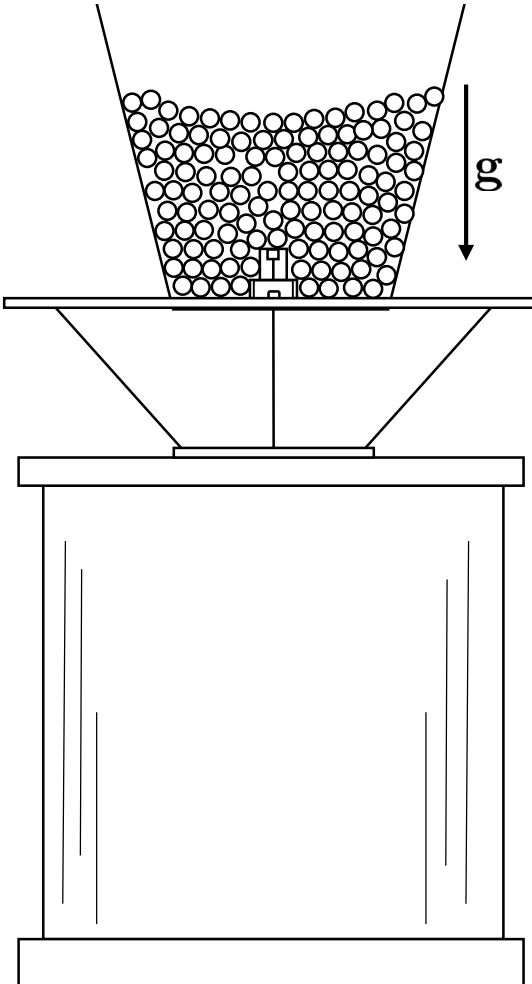


Solid lines->Modified Sonine
 Dashed lines->Standard Sonine
 Blue->vortices; Red->clusters
 Symbols: circles->vortices;
 triangles->clusters

P. Mitrano, VG, A. Hilger, C. Ewasko, C. Hrenya, PRE **85**, 041303 (2012)

In general, good agreement is observed between kinetic theory and MD simulations

Hydrodynamics of granular matter under vertical vibration



In most of the experimental situations, bottom plate is a **vibrating** plate while the top plate is open. System is in the presence of gravity. A steady state is achieved.

Hydrodynamic equations

$$\frac{\partial p}{\partial z} = -mng, \quad \frac{2}{dn} \frac{\partial}{\partial z} \left(\kappa \frac{\partial T}{\partial z} + \mu \frac{\partial n}{\partial z} \right) - T \zeta_0 = 0$$

Spatial gradients only along the z-direction

Measurements of Grain Motion in a Dense, Three-Dimensional Granular Fluid

Xiaoyu Yang, Chao Huan, and D. Candela

Physics Department, University of Massachusetts, Amherst, Massachusetts 01003

R. W. Mair and R. L. Walsworth

Harvard-Smithsonian Center for Astrophysics, Cambridge, Massachusetts 02138

(Received 16 August 2001; published 8 January 2002)

We have used an NMR technique to measure the short-time, three-dimensional displacement of grains in a system of mustard seeds vibrated vertically at 15g. The technique averages over a time interval in which the grains move ballistically, giving a direct measurement of the granular temperature profile. The dense, lower portion of the sample is well described by a recent hydrodynamic theory for inelastic hard spheres. Near the free upper surface the mean free path is longer than the particle diameter and the hydrodynamic description fails.

$$n^* = n\sigma^3, \quad z^* = z/\sigma, \quad T_{x,z}^* = T_{x,z}/mg\sigma, \quad \ell^* = \ell/\sigma$$

Free upper surface: saltation regime

[R. Chassagne, C. Bonamy, J. Chauchat, *J. Fluid Mech.* **964**, A27 (2023);
VG, *J. Fluid Mech.* **968**, F1 (2023)]

The smooth curves in Fig. 4 show a fit to the data of the hydrodynamic theory for inelastic hard spheres of Garzó and Dufty [4], which is applicable for wider ranges of density and inelasticity than other available theories. In

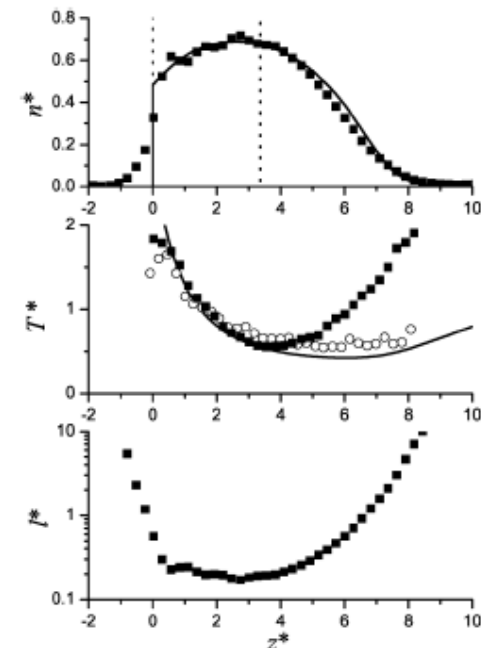


FIG. 4. (top) Measured dimensionless number density n^* (filled squares). (center) Measured dimensionless horizontal granular temperature T_x^* (filled squares) and vertical granular temperature T_z^* (open circles). (bottom) Dimensionless mean free path ℓ^* , computed from the density data. These quantities are plotted versus vertical position measured in grain diameters, $z^* = z/\sigma$. The smooth curves show the number density n^* and granular temperature T^* calculated from the theory of Ref. [4], with the heat current at sample bottom $q_z^*(0) = 3.4$ and restitution coefficient $\alpha = 0.90$ adjusted to fit the data. The vertical dotted lines in the top graph show the extent of the granular sample in the absence of vibration.

NMR experiments on a three-dimensional vibrofluidized granular medium

Chao Huan, Xiaoyu Yang,* and D. Candela

Physics Department, University of Massachusetts, Amherst, Massachusetts 01003, USA

R. W. Mair and R. L. Walsworth

Harvard-Smithsonian Center for Astrophysics, Cambridge, Massachusetts 02138, USA

(Received 27 May 2003; revised manuscript received 16 October 2003; published 29 April 2004)

A three-dimensional granular system fluidized by vertical container vibrations was studied using pulsed field gradient NMR coupled with one-dimensional magnetic resonance imaging. The system consisted of mustard seeds vibrated vertically at 50 Hz, and the number of layers $N_\ell \leq 4$ was sufficiently low to achieve a nearly time-independent granular fluid. Using NMR, the vertical profiles of density and granular temperature were directly measured, along with the distributions of vertical and horizontal grain velocities. The velocity distributions showed modest deviations from Maxwell-Boltzmann statistics, except for the vertical velocity distribution near the sample bottom, which was highly skewed and non-Gaussian. Data taken for three values of N_ℓ and two dimensionless accelerations $\Gamma = 15, 18$ were fitted to a hydrodynamic theory, which successfully models the density and temperature profiles away from the vibrating container bottom. A temperature inversion near the free upper surface is observed, in agreement with predictions based on the hydrodynamic parameter μ which is nonzero only in inelastic systems.

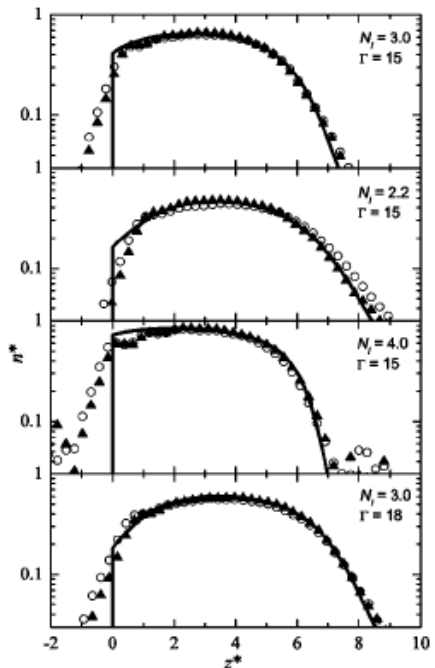


FIG. 14. Density profiles for the four different experimental conditions plotted on log-linear axes. These graphs show the same data as are shown in the top graphs of Figs. 10–13, using the same symbols. The hydrodynamic theory (curves) predicts a nearly exponential falloff of density with height z^* near the free upper surface (large z^*), resulting in straight lines on these semilog plots. The data (circles and triangles) generally agree with this prediction, but curve away from the theory curves at very low values of n^* due to the noise floor.

$$\alpha = 0.87$$

Good agreement between kinetic theory and experiments, except near the upper free surface

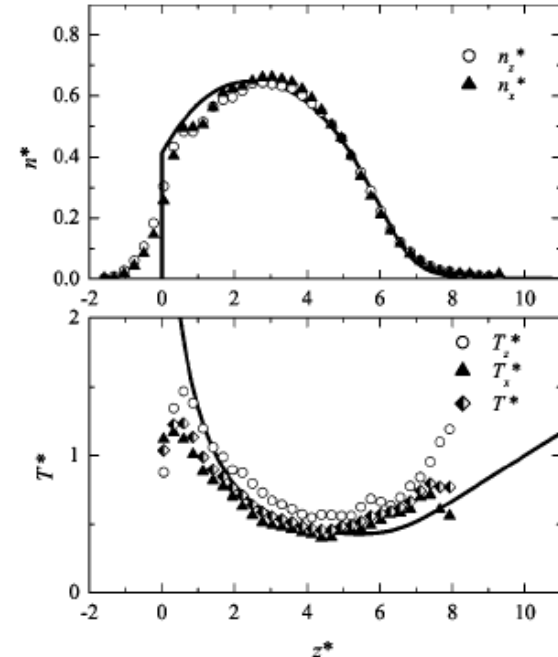


FIG. 10. Experimental density and granular temperature profiles (symbols) and fit to the hydrodynamic theory of Ref. [13] (curves) for $N_\ell = 3.0$ layers of grains vibrated at dimensionless acceleration amplitude $\Gamma = 15$. Dimensionless variables defined in Eq. (8) are used. In the top graph the symbols labeled n_z^* show the density profile $n^*(z^*)$ derived from the data set used to measure vertical displacements, while the symbols labeled n_x^* show the same quantity derived from the horizontal-displacement data set; these two profiles should be identical and differences reflect experimental accuracy. In the bottom graph T_z^* and T_x^* are the granular temperature profiles for vertical and horizontal displacements, respectively, measured using the observation interval $\Delta t = 1.38$ ms. It is expected that $T_z^* > T_x^*$, at least near the bottom of the sample, as energy is input only to the vertical degrees of freedom by the container vibration. The theory should be compared with the symbols labeled T^* , which are computed from the measured temperatures using $T^* = T_z^*/3 + 2T_x^*/3$.

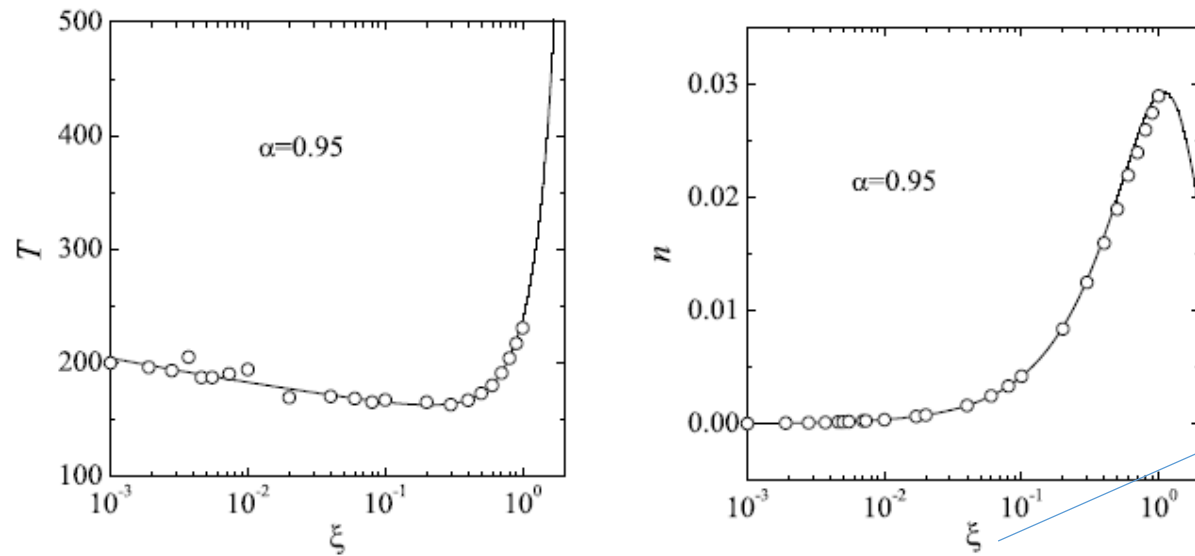
$$\alpha = 0.87$$

Dilute granular gas

Very nice analytical solution

[J. J. Brey et al. PRE **62**, 5339 (2000), PRE **63**, 061305 (2001)]

Temperature and density profiles given in terms of the modified Bessel functions



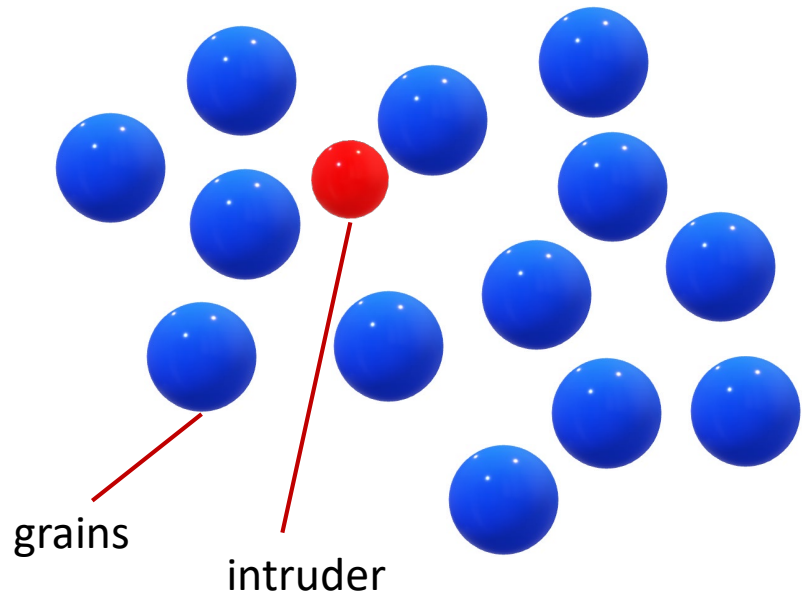
Significant role played by μ
in the inversion of the temperatura profile
near the free upper surface

Scaled variable (decreasing function of z)

DIFUSION OF AN INTRUDER IN A GRANULAR GAS IN HCS

Special case of a binary mixture: **tracer** limit

$$\left(c = \frac{n_0}{n + n_0} \rightarrow 0 \right)$$



Notation:

Intruder:	m_0, σ_0, α_0
Granular gas:	m, σ, α

- Granular gas (excess component) is not perturbed by the presence of tracer particles. It is in HCS
- Collisions among tracer particles can be also neglected in their kinetic equation
- Coefficients of restitution α, α_0

$$\frac{\partial f_{\text{HCS}}}{\partial t} = \chi J[f_{\text{HCS}}, f_{\text{HCS}}] \quad \text{Enskog kinetic equation}$$

$$\frac{\partial f_0}{\partial t} + \mathbf{v} \cdot \nabla f_0 = \chi_0 J_0[f_0, f_{\text{HCS}}] \quad \text{Enskog-Lorentz kinetic equation}$$

Goal: determine the (tracer) diffusion coefficient

Granular gas: HCS

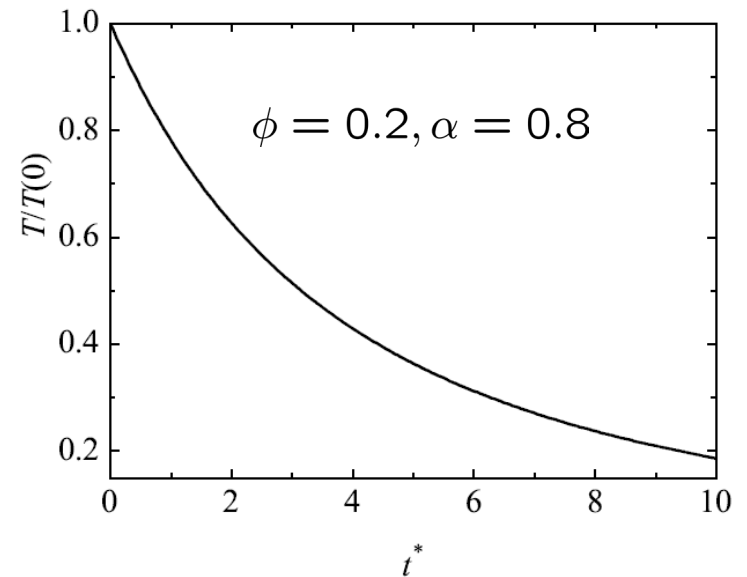
Energy balance equation $\frac{\partial T(t)}{\partial t} = -\zeta(t)T(t), \quad \zeta(T(t)) \propto \sqrt{T(t)}$

Haff's cooling law

$$T(t) = \frac{T(0)}{\left(1 + \frac{1}{2}\zeta(0)t\right)^2}$$

P. K. Haff, J. Fluid Mech. **134**, 401 (1983)

Haff's law has been shown to be robust in several experiments
[C.C. Maab et al., PRL **100**, 248001 (2008); S. Tatsumi et al., JFM **641**, 521 (2009);
K. Harth et al., PRL **110**, 144102 (2013); PRL **120**, 213301 (2018);
P. Yu et al., PRL **124**, 208007 (2020); Pitikaris et al. npjMicrogravity **8**, 11 (2022)]



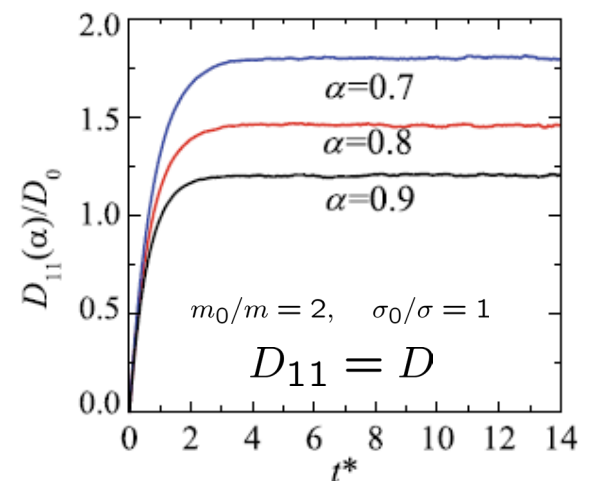
Diffusion of tracer species

Chapman-Enskog solution. Diffusion generated by a concentration gradient ∇n_0

Diffusion equation $\frac{\partial c}{\partial t} = D(t) \nabla^2 c, \quad c = n_0/n$

Hydrodynamic (normal) solution $D(t) = D_0(T(t)) D^*$

$$D_0(t) = \frac{T(t)}{m_0 \nu(t)}, \quad \nu(t) \propto \sqrt{T(t)}, \quad t^* = \nu(t)t$$



DSMC simulations

[J.M. Montanero, VG, PRE **69**, 021301 (2004)]

Time dependence of the diffusion equation can be eliminated

$$s = \int_0^t dt' \nu(t'), \quad \mathbf{r}' = \frac{\mathbf{r}}{\ell} \quad \nu(t) = \frac{16}{5} \sqrt{\pi n \sigma^2} \sqrt{T(t)/m}$$

$$\frac{\partial c}{\partial s} = \frac{m}{m_0} D^* \nabla_{\mathbf{r}'}^2 c$$

Standard diffusion equation with a **time-independent** diffusion coefficient

MSD of the intruder's position after a time interval s

$$\Delta \mathbf{r}' \equiv \mathbf{r}'(s) - \mathbf{r}'(0)$$

$$\frac{\partial}{\partial s} \langle |\Delta \mathbf{r}'|^2(s) \rangle = 2d \frac{m}{m_0} D^*$$

Going back to the original variables

$$\langle |\Delta \mathbf{r}|^2(t) \rangle = d \left[\frac{\Gamma\left(\frac{d}{2}\right)}{\Gamma\left(\frac{d+1}{2}\right)} \right]^2 \frac{2\nu(0)m}{m_0\zeta(0)} D^* \ln \left(1 + \frac{\zeta(0)}{2\nu(0)} t^* \right) \ell^2$$

E. Abad, S, Bravo Yuste, VG, Granular Matter **24**, 11 (2022)

For inelastic collisions, $(\alpha \neq 1, \alpha_0 \neq 1)$

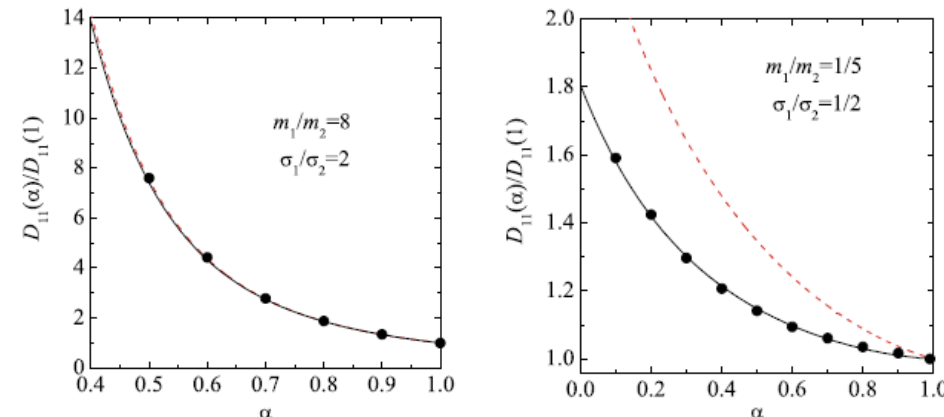
MSD increases **logarithmically** with time. **Ultraslow** diffusion

Our results extend previous works devoted to self-diffusion [J. J. Brey *et al.*, PF **12**, 876 (2000); N. Brilliantov, T. Pöschel, PRE **61**, 1716 (2000)] and Brownian limit [J. J. Brey *et al.*, PRE **60**, 7174 (1999)]

Approximate expressions for D^* . First (dashed lines) and second (solid lines) Sonine approximations.

DSMC simulations

[J.M. Montanero, VG, PRE **69**, 021301 (2004);
VG, F. Vega Reyes, PRE **79**, 041303 (2009)]



$$D^* = \frac{D_{11}(\alpha)}{D_{11}(1)}$$

Granular suspensions: **Normal** diffusion

[R. Gómez González, E. Abad, S. B. Yuste, VG, PRE **108**, 024903 (2023)]

INTRUDER'S MOTION AS A RANDOM WALK

Intruder's motion: succession of ballistic displacements \vec{r}_i interrupted by collisions with the granular gas

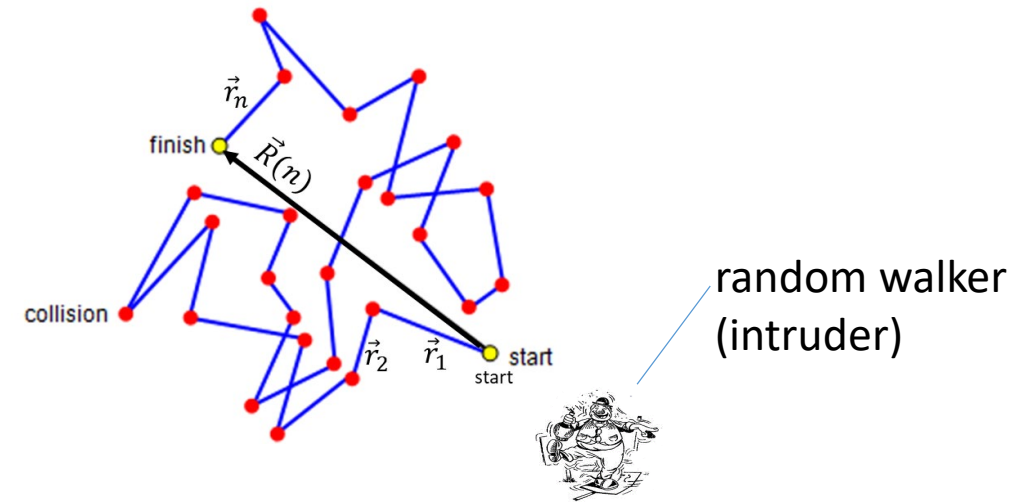
Deflection caused by each collision->**jump**

Succesion of jumps->**random walk** (RW)

$$\mathbf{R}(n) \equiv \vec{R}(n) = \vec{r}_1 + \vec{r}_2 + \dots = \sum_{i=1}^n \vec{r}_i$$

If the displacements (steps) \vec{r}_i between collisions are spatially homogeneous

$$\boxed{\langle \mathbf{R}^2(n) \rangle = n \langle r^2 \rangle + 2 \sum_{i < j} \langle \vec{r}_i \cdot \vec{r}_j \rangle} \quad \langle r^2 \rangle \simeq 2\ell_0^2, \quad \ell_0 \rightarrow \text{mean free path}$$



The evaluation of the second term is quite cumbersome because....

THE DISPLACEMENTS \vec{r}_i OF THE WALKER
ARE CORRELATED!!!!

Persistence: average fraction of the initial velocity that survives after a collision

As a first attempt..... as the steps of the RW were **isotropic**

$$\langle R^2(n) \rangle = n \ell_e^2 = s_0(t) \ell_e^2$$

“effective mean free path”

Average number of intruder-gas collisions (known quantity)

In particular $\langle \vec{r}_i \cdot \vec{r}_{i+1} \rangle > 0$ (the microscopic collision rules cause the *postcollisional displacement* of the intruder to have, on average, a significant component in the direction of the *precollisional displacement*: there is **persistence!**)

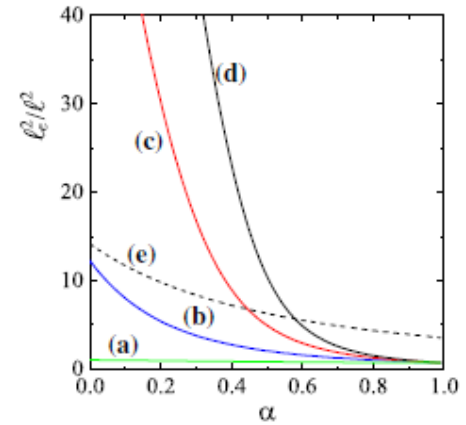


Fig. 5 Plot of the square effective length ℓ_e^2/ℓ^2 scaled with the mean free path of the gas particles versus the (common) coefficient of normal restitution $\alpha = \alpha_0$. The solid lines correspond to the four different cases depicted in Fig. 3, namely, $m_0/m = 0.5$ (a), $m_0/m = 5$ (b), $m_0/m = 8$ (c), and $m_0/m = 10$ (d). In all four cases, the diameter ratio is $\sigma_0/\sigma = 2$. The dashed line (e) corresponds to the self-diffusion case with $m_0/m = 1$ and $\sigma_0/\sigma = 1$.

E. Abad, S. Bravo Yuste, VG, Granular Matter 24, 11 (2022)

Let's go back to the difficult problem.....

Based on arguments given for molecular gases in very old papers [L. M. Yang, Proc. R. Soc. Lond A 198, 94 (1949); W. H. Furry, P. H. Pitkanen, JCP 19, 729 (1951), L. Monchik, PF 5, 1393 (1962)].....

$$\begin{aligned}\langle R^2(n) \rangle &\approx 2n\ell_0^2 + 2n\langle \mathbf{r}_1 \cdot \mathbf{r}_2 \rangle + 2n\langle \mathbf{r}_1 \cdot \mathbf{r}_3 \rangle + \dots \\ &\approx 2n\ell_0^2 + 2n\ell_0^2 (\langle \cos \theta \rangle + \langle \cos \theta \rangle^2 + \dots) \\ &= \frac{2n\ell_0^2}{1 - \langle \cos \theta \rangle}\end{aligned}$$

(S. Bravo Yuste, unpublished)

$$\langle \cos \theta \rangle \equiv \langle \cos \theta \rangle = \langle \cos(\mathbf{r}, \mathbf{r}') \rangle = \langle \cos(\mathbf{v}_0, \mathbf{v}'_0) \rangle$$

After some calculations.....

(S. Bravo Yuste, VG, unpublished)

$$\langle \omega \rangle \approx 1 - \frac{1}{2} \frac{1 + \alpha_0}{1 + m_0/m} [1 - h(\theta)]$$

persistence

$$\langle \cos \rangle \approx \frac{\langle \omega \rangle}{\langle v'_0/v_0 \rangle}$$

$$\left\langle \frac{v'_0}{v_0} \right\rangle \approx \frac{4d\gamma - (1 - \alpha^2)}{4d\gamma + 1 - \alpha^2}$$

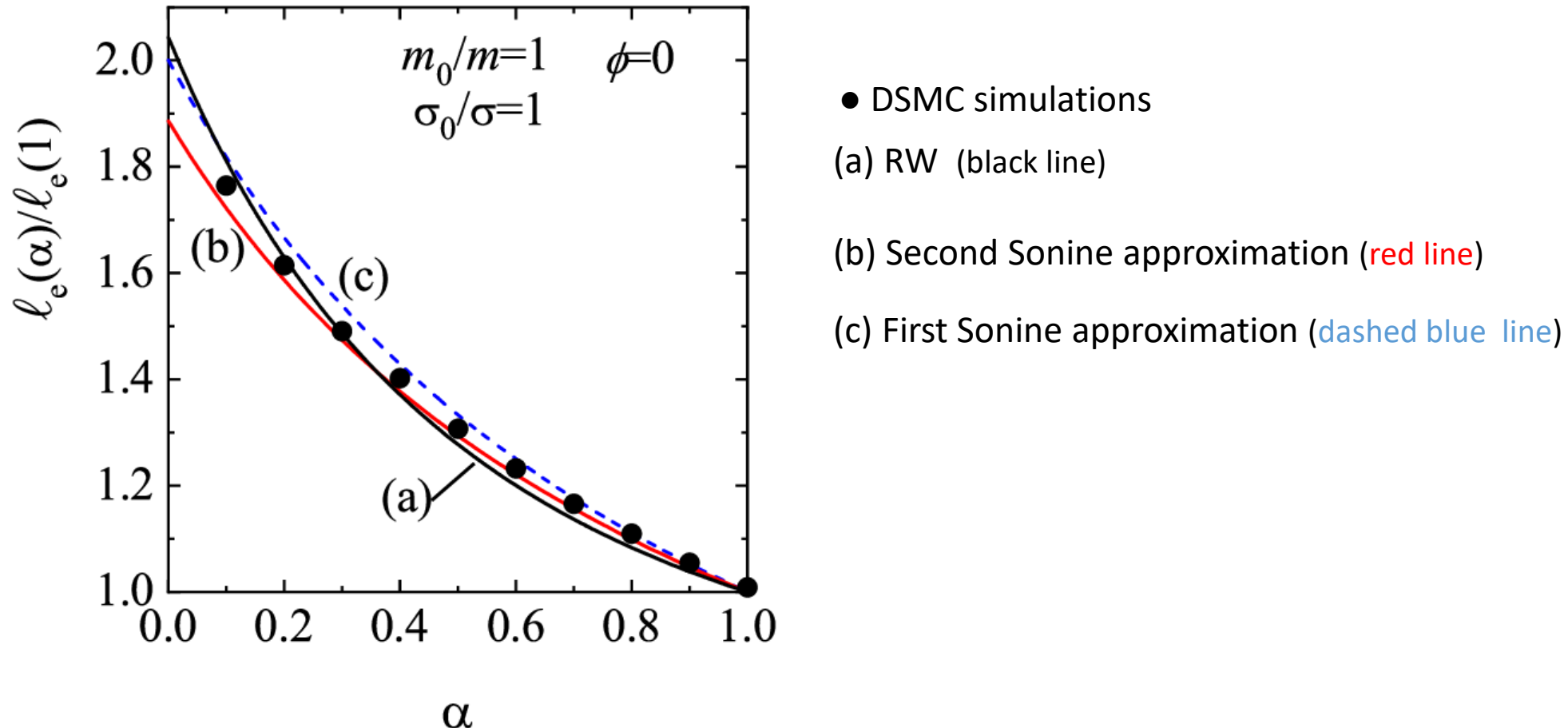
$$\theta = \frac{m_0 T}{m T_0}, \quad \gamma = \left(\frac{\sigma + \sigma_0}{2\sigma} \right)^{d-1} \frac{\chi_0}{\chi} \left(\frac{1 + \theta}{2\theta} \right)^{1/2}, \quad h(x) = \frac{x}{2} \left[\frac{x}{\sqrt{1+x}} \ln \left(\frac{1 + \sqrt{1+x}}{\sqrt{x}} \right) - 1 \right]$$

For elastic collisions, ($\alpha = \alpha_0 = 1, T = T_0, \langle v'_0/v_0 \rangle = 1$) we recover previous (old) results
(Chapman&Cowling textbook, 1970)

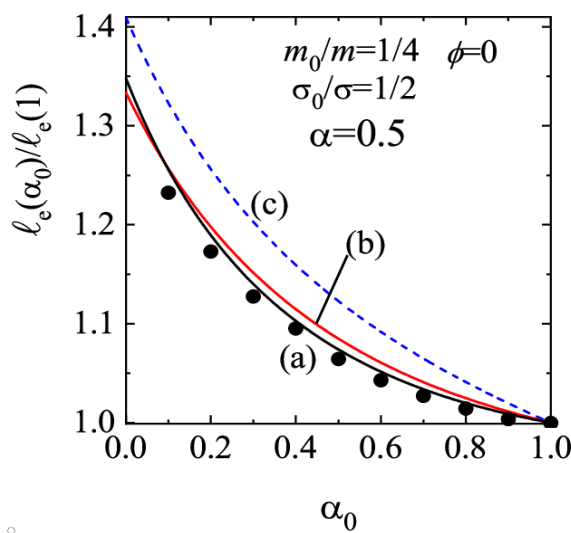
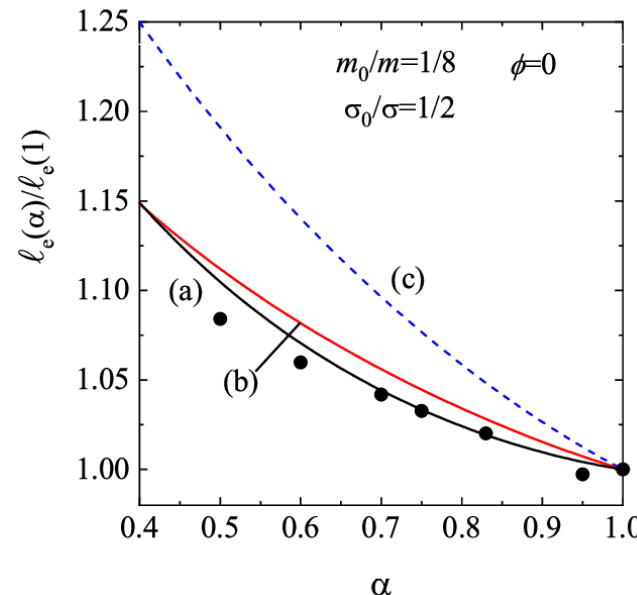
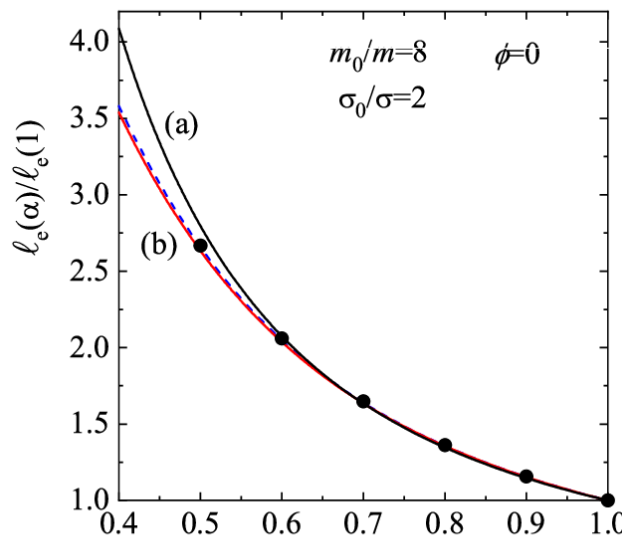
Self-diffusion $\langle \omega \rangle \approx 0.406$

$$\langle R^2(n) \rangle_{\text{RW}} = n \ell_e^2$$

Self-diffusion



$$\alpha = \alpha_0$$



$$\alpha_0 \neq \alpha = 0.5$$

● DSMC simulations

(a) RW (black line)

(b) Second Sonine approximation (red line)
(c) First Sonine approximation (dashed blue line)

RW results are surprisingly good !!!!

CONCLUSIONS

- Kinetic theory as a valuable tool for describing granular flows
- Controversy on the hydrodynamics-like type of description for strong inelasticity. Kinetic theory goes beyond the quasielastic limit
- Good agreement in general with DSMC simulations and even with MD simulations (impact of breakdown of molecular chaos hypothesis does not play a significant role in some macroscopic properties)
- It is also able to reproduce the hydrodynamic profiles in the bulk domain observed in real experiments of vibrating granular systems
- RW can be also a reliable tool to understand diffusion in granular gases. RW results are surprisingly good and excellent in some cases (especially when the ratio m_0/m is small)
- Possible **open** problems: include **roughness** in the kinetic theory description [Dilute monocomponent limit, G. Kremer, A. Santos, VG PRE **90**, 022205 (2014)]

ACKNOWLEDGMENTS



Prof. James W. Dufty
(University of Florida)



Prof. Christine H. Hrenya
(University of Colorado)



Dr. Peter Mitrano
(University of Colorado)



Andrés Santos
(UEx)



José María Montanero
(UEx)



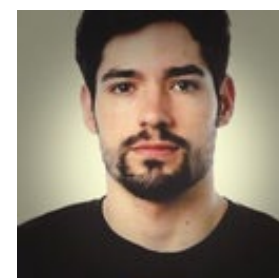
F. Vega Reyes
(UEx)



Santos Bravo Yuste
(UEx)



Enrique Abad
(UEx)



Rubén Gómez González
(UEx)